

Laser Frequency Combs for Astronomical Observations

Tilo Steinmetz,^{1,2} Tobias Wilken,¹ Constanza Araujo-Hauck,³ Ronald Holzwarth,^{1,2} Theodor W. Hänsch,¹ Luca Pasquini,³ Antonio Manescau,³ Sandro D'Odorico,³ Michael T. Murphy,⁴ Thomas Kentischer,⁵ Wolfgang Schmidt,⁵ Thomas Udem^{1*}

A direct measurement of the universe's expansion history could be made by observing in real time the evolution of the cosmological redshift of distant objects. However, this would require measurements of Doppler velocity drifts of ~ 1 centimeter per second per year, and astronomical spectrographs have not yet been calibrated to this tolerance. We demonstrate the first use of a laser frequency comb for wavelength calibration of an astronomical telescope. Even with a simple analysis, absolute calibration is achieved with an equivalent Doppler precision of ~ 9 meters per second at ~ 1.5 micrometers—beyond state-of-the-art accuracy. We show that tracking complex, time-varying systematic effects in the spectrograph and detector system is a particular advantage of laser frequency comb calibration. This technique promises an effective means for modeling and removal of such systematic effects to the accuracy required by future experiments to see direct evidence of the universe's putative acceleration.

Recent cosmological observations suggest that the universe's expansion is accelerating. Several lines of evidence corroborate this, including results from distant supernovae (1, 2), the cosmic microwave background (3), and the clustering of matter (4, 5). However, the current observations are all essentially geometric in nature, in that they map out space, its curvature, and its evolution. In contrast, a direct and dynamical determination of the universe's expansion history is possible by observing the slow drift of cosmological redshifts, z , that is inevitable in any evolving universe (6). No particular cosmological model or theory of gravity would be needed to interpret the results of such an experiment. However, the cosmological redshift drift is exceedingly small and difficult to measure; for currently favored models of the universe, with a cosmological constant parametrizing the acceleration, the redshifts of objects drift by less than $\sim 1 \text{ cm s}^{-1} \text{ year}^{-1}$ (depending on their redshifts).

Nevertheless, the suggestion that the so-called Lyman- α "forest" seen in high-redshift quasar spectra is the best target for this experiment (7) was recently supported by cosmological hydrodynamical simulations (8). The forest of absorption lines is caused by the Lyman- α transition arising in neutral hydrogen gas clouds at different redshifts along the quasar sight-lines. Detailed calculations with simulated quasar spectra show

that the planned 42-m European Extremely Large Telescope (E-ELT), equipped with the proposed Cosmic Dynamics Experiment (CODEX) spectrograph (9), could detect the redshift drift convincingly with 4000 hours of observing time over

a ~ 20 -year period (8). Therefore, as the observation is feasible (in principle), overcoming the many other practical challenges in such a measurement is imperative. Important astrophysical and technical requirements have been considered in detail, and most are not difficult to surmount (8, 10). One (but not the only) extremely important requirement is that the astronomical spectrographs involved must have their wavelength scales calibrated accurately enough to record $\sim 1 \text{ cm s}^{-1}$ velocity shifts (~ 25 -kHz frequency shifts) in the optical range. Moreover, this accuracy must be repeatable over ~ 20 -year time scales.

Although the redshift drift experiment requires demanding precision and repeatability, precisely calibrated astronomical spectrographs have several other important applications. For example, Jupiter- and Neptune-mass extrasolar planets have been discovered by the reflex Doppler motion of their host stars (11–13), but detecting Earth-mass planets around solar-mass stars will require $\sim 5 \text{ cm s}^{-1}$ precision maintained over several-year time scales (14). Another example is the search for shifts in narrow quasar absorption lines caused by cosmological variations in the fundamental constants of nature (15–17). Recent measurements (18–21) achieve precisions of $\sim 20 \text{ m s}^{-1}$, but the possibility of hidden systematic effects, and the increased photon-collecting power of future ELTs, warrant

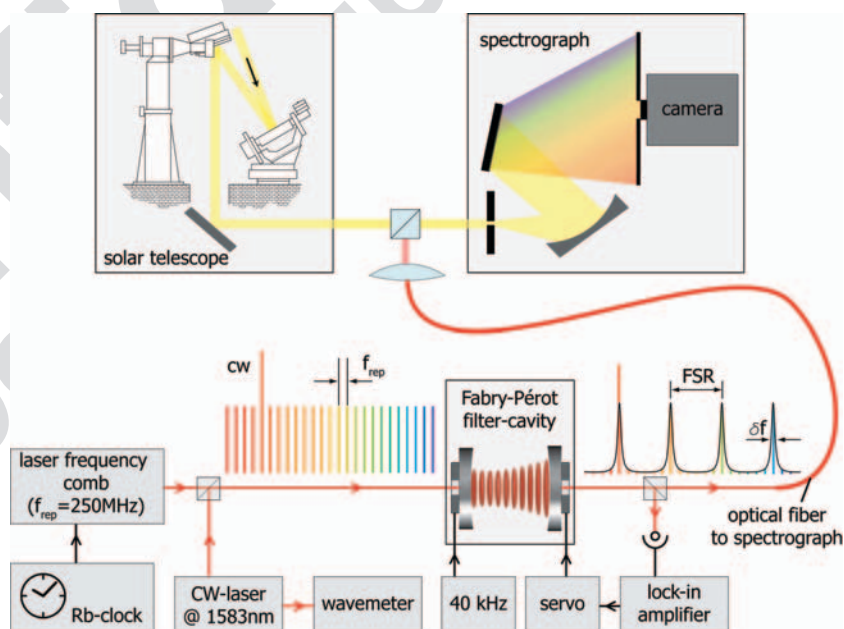


Fig. 1. Sketch of our experimental setup at the VTT. By superimposing the frequency comb with light from a celestial body—in this case, the Sun—one can effectively calibrate its emission or absorption spectrum against an atomic clock. An erbium-doped fiber LFC with 250-MHz mode spacing (pulse repetition rate) is filtered with a FPC to increase the effective mode spacing, allowing it to be resolved by the spectrograph. The latter has a resolution of ~ 0.8 GHz at wavelengths around $1.5 \mu\text{m}$, where our LFC tests were conducted. The LFC was controlled by a rubidium atomic clock. A continuous-wave (CW) laser at 1583 nm was locked to one comb line and simultaneously fed to a wavemeter. Even though the wavemeter is orders of magnitude less precise than the LFC itself, it is sufficiently accurate (better than 250 MHz) to identify the mode number, n . The FPC length, defining the final free spectral range (FSR), was controlled by feedback from its output. See (10) for further details.

¹Max-Planck für Quantenoptik, Hans-Kopfermann-Strasse 1, D-85748 Garching, Germany. ²Menlo Systems GmbH, Am Klopferspitz 19, D-82152 Martinsried, Germany. ³European Southern Observatory, Karl-Schwarzschild-Strasse 3, D-85748 Garching, Germany. ⁴Centre for Astrophysics and Supercomputing, Swinburne University of Technology, Mail H39, Post Office Box 218, Victoria 3122, Australia. ⁵Kiepenheuer-Institut für Sonnenphysik, Schönebeckstr. 6, D-79104 Freiburg, Germany.

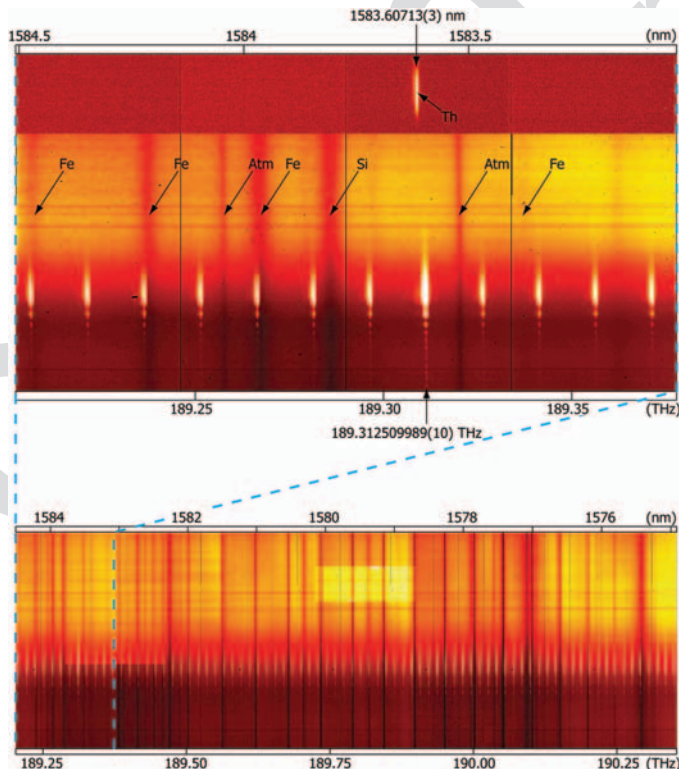
*To whom correspondence should be addressed. E-mail: thu@mpq.mpg.de

much more precise and accurate calibration over the widest possible wavelength range.

Laser frequency combs (LFCs) offer a solution because they provide an absolute, repeatable wavelength scale defined by a series of laser modes equally spaced across the spectrum. The train of femtosecond pulses from a mode-locked laser occurs at the pulse repetition rate, f_{rep} , governed by the adjustable laser cavity length. In the frequency domain, this yields a spectrum, $f_n = f_{\text{ceo}} + (n \times f_{\text{rep}})$, with modes enumerated by an integer $n \sim 10^5$ to 10^6 . The carrier envelope offset frequency, $f_{\text{ceo}} \leq f_{\text{rep}}$, accounts for the laser's internal dispersion, which causes the group and phase velocities of the pulses to differ (22). Thanks to the large integer n , the optical frequencies f_n are at hundreds of THz whereas both f_{rep} and f_{ceo} are radio frequencies and can be handled with simple electronics and stabilized by an atomic clock (22). Each mode's absolute frequency is known to a precision limited only by the accuracy of the clock. Even low-cost, portable atomic clocks provide $\sim 1 \text{ cm s}^{-1}$ (or 3 parts in 10^{11}) precision. Because LFC light power is much higher than required, the calibration precision possible is therefore limited by the maximum signal-to-noise ratio (SNR) achievable with the detector. For modern astronomical charge-coupled devices (CCDs), the maximum SNR in a single exposure is limited by their dynamic range but is still sufficient to achieve $\sim 1 \text{ cm s}^{-1}$ precision (23). Furthermore,

Fig. 2. Spectra of the solar photosphere (background image) overlaid by a LFC with 15-GHz mode spacing (white, equally spaced vertical stripes). Spectra are dispersed horizontally, whereas the vertical axis is a spatial cross section of the Sun's photosphere. The upper panel shows a small section of the larger portion of the spectrum below. The brighter mode labeled with its absolute frequency is additionally superimposed with a CW laser used to identify the mode number (Fig. 1). The frequencies of the other modes are integer multiples of 15 GHz higher (right) and lower (left) in frequency. Previous calibration methods would use the atmospheric absorption lines (dark vertical bands labeled "Atm" interleaved with the Fraunhofer

absorption lines), which are comparably few and far between. Also shown in the upper panel is the only thorium emission line lying in this wavelength range from a typical hollow-cathode calibration lamp. Recording it required an integration time of 30 min, compared with the LFC exposure time of just 10 ms. Unlike with the LFC, the thorium calibration method cannot be conducted simultaneously with solar measurements at the VTT. The nominal horizontal scale is $1.5 \times 10^{-3} \text{ nm pixel}^{-1}$ with ~ 1000 pixels shown horizontally in the upper panel. Black horizontal and vertical lines are artifacts of the detector array.



because LFC calibration is absolute, spectra from different epochs, or even different telescopes, can be meaningfully compared.

The main challenge in reaching $\sim 1 \text{ cm s}^{-1}$ calibration accuracy will be the measurement and, eventually, mitigation and/or modeling and removal of systematic effects in astronomical spectrographs and detectors. For typical high-resolution spectrographs, a $\sim 1 \text{ cm s}^{-1}$ shift corresponds roughly to the physical size of a silicon atom in the CCD substrate. Only with the statistics of a very large number of calibration lines can the required sensitivity be achieved, provided that systematic effects can be controlled accordingly (10). For example, even in a highly stabilized, vacuum-sealed spectrograph, small mechanical drifts will slightly shift the spectrum across the CCD. Although this can easily be tracked to first order, other effects such as CCD intrapixel sensitivity variations will be important for higher precision. Discovering, understanding, and eventually modeling and removing these effects is crucial for the long-term goal of accurate calibration; tests of LFCs on astronomical telescopes, spectrographs, and detectors are therefore imperative.

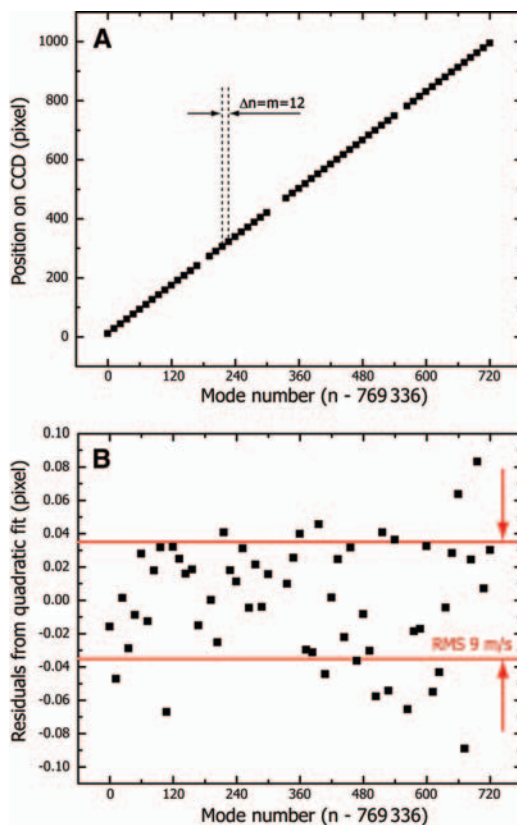
We have conducted an astronomical LFC test on the German Vacuum Tower Telescope (24) (VTT) (Fig. 1). We used a portable rubidium clock with a modest accuracy of 5 parts in 10^{11} (or 1.5 cm s^{-1}); much more accurate clocks are

available if needed. This sets the absolute uncertainty on the frequency of any given comb mode. The VTT can be operated at near-infrared wavelengths, thereby allowing a relatively simple and reliable fiber-based LFC to be used. The erbium-doped fiber LFC used had $f_{\text{rep}} = 250 \text{ MHz}$ which, despite the VTT spectrograph having higher resolving power (resolution of 0.8 GHz or 1.2 km s^{-1}) than most astronomical spectrographs, is too low for modes to be resolved apart. Filtering out unwanted modes by using a Fabry-Pérot cavity (FPC) outside the laser (25, 26) was suggested as one solution (23, 27) and has proven effective (28, 29). The FPC comprises two mirrors separated by a distance smaller than the laser cavity length so that all modes, except every m th ($m > 1$), are interferometrically suppressed (Fig. 1, lower panel). We used a FPC stabilized to a filter ratio, m , by controlling its length with an electronic servo system to generate effective mode spacings, $m \times f_{\text{rep}}$, between 1 and 15 GHz. The degree to which the unwanted modes are suppressed is an important parameter: The FPC transmission function falls sharply away from the transmitted mode frequencies but, because nearby suppressed modes are not resolved from the transmitted ones by the spectrograph, small asymmetries in this function (especially combined with time variations) can cause systematic shifts in the measured line positions. With our setup, we achieve an unwanted mode suppression of more than 46 dB at filter ratios $m \leq 20$. Other possible systematic shifts due to the filtering have been identified (29) and need to be controlled.

LFC spectra were recorded with and without the spectrum of a small section of the Sun's photosphere at wavelengths $\sim 1.5 \mu\text{m}$. A sample $m \times f_{\text{rep}} = 15\text{-GHz}$ recording, superimposed with Fraunhofer and atmospheric lines, is shown in Fig. 2. To estimate our calibration accuracy and to test the spectrograph's stability, we analyzed several exposures of the LFC only. Individual Lorentzian functions were fitted to the recorded modes as a function of pixel position and identified with the absolute comb frequencies, f_n , which are referenced to the atomic clock (10). The dense grid of modes allows the spectrograph's calibration function (Fig. 3A) to be determined to very high accuracy; even a simple, second-order polynomial fit to the pixel-versus-frequency distribution has only 9 m s^{-1} root mean square (RMS) residual deviations around it (Fig. 3B), and this remains almost unchanged with higher-order polynomial modeling (10).

With traditional calibration techniques, such as thorium comparison lamps, I_2 gas absorption cells or Earth's atmospheric absorption lines for calibration achieve $\sim 10 \text{ m s}^{-1}$ absolute precision per calibration line at best (30). Thus, even with these "first light" comb recordings, we already demonstrate superior absolute calibration accuracy. Because more than 10^4 modes will be available in a larger-bandwidth LFC, the statistical uncertainty would be reduced to the 1 cm s^{-1} regime if the residuals were truly random. However, the theoretical shot noise limit calculated from the

Fig. 3. Precision achieved with our calibration with a LFC filtered to 3 GHz ($m = 12$). **(A)** The position of the transmitted modes, derived from a multi-Lorentzian fit, plotted against the mode number. Modes without a corresponding detector position measurement were deemed unsuitable for use in calibration because they fell on large detector artifacts and/or were overlaid with light from the CW laser. The size of one pixel corresponds to 172 MHz at 1583 nm. On this scale, no distortions are visible. **(B)** The residuals from a quadratic fit that gives a RMS residual of 9 m s^{-1} . The quadratic fit greatly reduces the residuals compared to a linear model, whereas higher-order polynomials do not improve the performance of the fit significantly (10). Even with these first LFC recordings from the VTT, the 9 m s^{-1} RMS residuals here indicate better absolute calibration than is achieved with traditional calibration methods (30).



number of photons recorded per comb mode is much smaller than 9 m s^{-1} ; systematic effects from the spectrograph and detector system evidently completely dominate the residuals.

The main reason for testing LFCs at real telescopes, on real astronomical spectrograph and detector systems, is to understand how to measure and then mitigate and/or model and remove such systematics. Because the VTT spectrograph is not stabilized (i.e., temperature-, pressure- and vibration-isolated), instrument drifts are expected and the VTT LFC spectra can already be used to track them accurately. From a time series of exposures, we derive a drift in the spectrograph of typically $8 \text{ m s}^{-1} \text{ min}^{-1}$ (5 MHz min^{-1}) (10). Much lower drift rates have been demonstrated with suitably stabilized instruments [e.g., $\sim 1 \text{ m s}^{-1}$ over months with HARPS (13)]; although the VTT is not optimized for stability, this does not affect its usefulness to test calibration procedures. Indeed, different modes are observed to drift at different rates, with neighboring modes having

highly correlated drift rates (10). Also, as the comb modes drift across the detector, higher-order distortions are evident, which are the combined result of many effects, such as intrapixel sensitivity variations. Thus, the VTT data already show an important advantage of LFC calibration: The dense grid of high SNR calibration information allows the discovery and measurement of complex effects correlated across the chip and in time.

The first light for frequency combs on astronomical spectrographs has delivered calibration precision beyond the state of the art. The key opportunity now is to use LFC spectra to measure and remove systematic effects in order to reach the $\sim 1 \text{ cm s}^{-1}$ long-term calibration precision, accuracy, and repeatability required to realize the redshift drift experiment.

References and Notes

1. A. G. Riess *et al.*, *Astron. J.* **116**, 1009 (1998).
2. S. Perlmutter *et al.*, *Astrophys. J.* **517**, 565 (1999).
3. D. N. Spergel *et al.*, *Astrophys. J.* **148**, (Suppl.), 175 (2003).

4. J. A. Peacock *et al.*, *Nature* **410**, 169 (2001).
5. D. J. Eisenstein *et al.*, *Astrophys. J.* **633**, 560 (2005).
6. A. Sandage, *Astrophys. J.* **136**, 319 (1962).
7. A. Loeb, *Astrophys. J.* **499**, L111 (1998).
8. J. Liske *et al.*, *Mon. Not. R. Astron. Soc.* **386**, 1192 (2008).
9. L. Pasquini *et al.*, in *Proceedings of the IAU Symposium*, P. Whitelock, M. Dennefeld, B. Leibundgut, Eds. (Cambridge Univ. Press, Cambridge, UK, 2006), vol. 232, pp. 193–197.
10. Materials and methods are available as supporting material on Science Online.
11. M. Mayor, D. Queloz, *Nature* **378**, 355 (1995).
12. G. W. Marcy, R. P. Butler, *Astrophys. J.* **464**, L147 (1996).
13. C. Lovis *et al.*, *Nature* **441**, 305 (2006).
14. C. Lovis *et al.*, in *Proceedings of the SPIE*, I. S. McLean, I. Masanori, Eds. (2006), vol. 6269, pp. 62690P1–9.
15. J. N. Bahcall, E. E. Salpeter, *Astrophys. J.* **142**, 1677 (1965).
16. J. K. Webb, V. V. Flambaum, C. W. Churchill, M. J. Drinkwater, J. D. Barrow, *Phys. Rev. Lett.* **82**, 884 (1999).
17. R. I. Thompson, *Astron. Lett.* **16**, 3 (1975).
18. M. T. Murphy, J. K. Webb, V. V. Flambaum, *Mon. Not. R. Astron. Soc.* **345**, 609 (2003).
19. H. Chand, R. Srianand, P. Petitjean, B. Aracil, *Astron. Astrophys.* **417**, 853 (2004).
20. S. A. Levshakov *et al.*, *Astron. Astrophys.* **449**, 879 (2006).
21. E. Reinhold *et al.*, *Phys. Rev. Lett.* **96**, 151101 (2006).
22. Th. Udem, R. Holzwarth, T. W. Hänsch, *Nature* **416**, 233 (2002).
23. M. T. Murphy *et al.*, *Mon. Not. R. Astron. Soc.* **380**, 839 (2007).
24. E. H. Schröter, D. Soltau, E. Wiehr, *Vistas Astron.* **28**, 519 (1985).
25. T. I. Sizer, *IEEE J. Quantum Electron.* **25**, 97 (1989).
26. Th. Udem, J. Reichert, R. Holzwarth, T. W. Hänsch, *Phys. Rev. Lett.* **82**, 3568 (1999).
27. P. O. Schmidt, S. Kimeswenger, H. U. Kaeufl, *Proc. 2007 ESO Instrument Calibration Workshop*, ESO Astrophysics Symposia series (Springer, in press); available at <http://arxiv.org/abs/0705.0763>.
28. C.-H. Li *et al.*, *Nature* **452**, 610 (2008).
29. D. A. Braje, M. S. Kirchner, S. Osterman, T. Fortier, S. A. Diddams, *Eur. Phys. J. D* **48**, 57 (2008).
30. C. Lovis, F. Pepe, *Astron. Astrophys.* **468**, 1115 (2007).
31. We thank the Kiepenheuer Institut für Sonnenphysik staff at the Vacuum Tower Telescope and the Instituto de Astrofísica de Canarias (IAC) personnel for their support during the measurements at the VTT. We especially appreciate the efforts of M. Collados (IAC) and F. Kerber (ESO). We thank T. Kippenberg for CW-laser assistance and J. Liske for advice on the manuscript. M.T.M. thanks the Australian Research Council for a QEII Research Fellowship (DP0877998).

Supporting Online Material

www.sciencemag.org/cgi/content/full/1161030/DC1
Materials and Methods
Figs. S1 to S4
References

28 May 2008; accepted 25 July 2008
10.1126/science.1161030